Magnetism of the chromium thio-spinels $Fe_{1-x}Cu_xCr_2S_4$ studied using muon spin rotation and relaxation

G M Kalvius[1], A Krimmel[2], R Wäppling[3], O Hartmann[3], F J Litterst[4], F E Wagner[1], V Tsurkan[2,5] and A Loidl[2]

[1] Physics Department, Technical University Munich, D-85747 Garching, Germany
[2] Experimental Physics V, Center for Electronic Correlations and Magnetism, Augsburg University, D-86159 Augsburg, Germany
[3] Department of Physics and Astronomy, Uppsala University, D-75120 Uppsala, Sweden
[4] Institute for Physics of Condensed Matter, Technical University Braunschweig, D-38106 Braunschweig, Germany
[5] Institute of Applied Physics, Academy of Sciences, 2028 Chisinau, Republic of Moldova

E-mail: roger.wappling@fysik.uu.se

Abstract

Powder samples of $Fe_{1-x}Cu_xCr_2S_4$ with $x = 0, 0.2, 0.5, 0.8$ were studied, between 5 and 300 K. The results reveal that for $x < 1$, the magnetic order in the series is more varied than the simple collinear ferrimagnetic structure traditionally assumed to exist everywhere from the Curie point to $T \to 0$. In $FeCr_2S_4$ several ordered magnetic phases are present, with the ground state likely to have an incommensurate cone-like helical structure. $Fe_{0.8}Cu_{0.2}Cr_2S_4$ is the compound for which simple collinear ferrimagnetism is best developed. In $Fe_{0.5}Cu_{0.5}Cr_2S_4$ the ferrimagnetic spin structure is not stable, causing spin reorientation around 90 K. In $Fe_{0.2}Cu_{0.8}Cr_2S_4$ the ferrimagnetic structure is at low temperatures considerably distorted locally, but with rising temperature this disorder shows a rapid reduction, coupled to increased spin fluctuation rates. In summary, the present data show that the changes induced by the replacement of Fe by Cu have more profound influences on the magnetic properties of the $Fe_{1-x}Cu_xCr_2S_4$ compounds than merely a shift of Curie temperature, saturation magnetization and internal field magnitude.

1. Introduction

Features like colossal magnetoresistance (CMR) have made chromium based spinels a target of intensive research for many years [1]. In the normal spinel structure AB_2X_4, the A-site ions with nominal valence 2+ are tetrahedrally coordinated and the B-site ions with nominal valence 3+ are octahedrally coordinated with the X ions, which can be oxygen, sulfur or selenium in the 2− charge state [2, 3]. On either site, magnetic ions experience frustration. In the diamond sublattice formed by the A-site ions, frustration originates from competing interactions between nearest and next nearest exchange couplings [4, 5]. The pyrochlore structure of the B-site ions is a three-dimensional geometrically frustrated lattice [6, 7]. In general, frustration tends to suppress magnetic long-range order (LRO). In particular, collinear antiferromagnetic spin structures are usually unstable. Another characteristic feature is that the magnetic spins exhibit strong fluctuations. They ease frustration and are often persistent in the limit $T \to 0$ [8].

$FeCr_2S_4$ and $CuCr_2S_4$ both crystallize in the normal spinel structure with lattice constants $a = 9.995$ Å (Fe) and $a = 9.814$ Å (Cu) at 300 K [9]. This allows one to synthesize the whole range of solid solutions $Fe_{1-x}Cu_xCr_2S_4$ with the lattice constant roughly following Vegard's law [10, 11]. More of a problem is the charge compensation [2, 3, 12].

In the concentration range $0 \leq x \leq 0.5$ the situation is fairly straightforward. One finds

$$(Fe^{2+}_{1-2x}Fe^{3+}_{x}Cu^{+}_{x})[Cr^{3+}_{2}]S^{2-}_{4}.$$

For $x > 0.5$, iron is always in the 3+ state, while the charge state of chromium is a matter of controversy. In [2], charge compensation is considered to occur via an appropriate mixture of Cr^{3+} and Cr^{4+} together with holes (S^{-}) in the valence band, whereas copper is kept in the monovalent state throughout:

$$(Fe^{3+}_{1-x}Cu^{+}_{x})[Cr^{3+}_{3-2x+\delta}Cr^{4+}_{2x-1-\delta}]S^{2-}_{4-\delta}S^{-}_{\delta}.$$

In [3] it is assumed that chromium is always trivalent, but that copper can be partially divalent:

$$(Fe^{3+}_{1-x}Cu^{+}_{1-x}Cu^{2+}_{2x-1})[Cr^{3+}_{2}]S^{2-}_{4}.$$

Theoretical treatments depend on whether more ionic or more covalent bonding is assumed. A recent study of the valence states of Fe, Cu, and Cr by photoelectron and x-ray absorption spectroscopy using synchrotron radiation [13] found that Cu and Cr remain in the same valence state throughout the series, indicating that charge compensation must predominantly occur via valence band holes. Additional evidence for that picture was reported in [14].

$FeCr_2S_4$ is a semiconductor developing magnetic LRO around 170 K. Early powder neutron diffraction data [15, 16], which were taken only at 4.2 and 300 K and hence lacked a full temperature dependence, reported the LRO spin structure to be a collinear ferrimagnet based on antiferromagnetically coupled ferromagnetic Fe and Cr sublattices with ordered moments $\mu_{Fe} = 4.2\ \mu_B$ and $\mu_{Cr} = 2.9\ \mu_B$. In contrast, $CuCr_2S_4$ is metallic and a ferromagnet with $T_C = 376$ K, meaning that the A-site Cu ions are in a nonmagnetic state. Early on, Mössbauer spectroscopy for $FeCr_2S_4$ found a sudden change of hyperfine parameters below ∼10 K, indicating a static Jahn–Teller transition [17]. This transition into an ordered orbital ground state was later studied in detail [18]. At this point, it should be mentioned that the presence of slight disorder (produced for example by weak doping in single crystals grown with chlorine gas as the transport agent) suppresses this transition, and the ground state is then characterized by the freezing of the orbital moments into an orbital glass [19]. In the neutron studies [15, 16] it was further stated that the cubic spinel structure is maintained at 4.2 K. This result was later challenged for the temperature range below ∼60 K by transmission electron [20] and ultrasound [21] studies. On the basis of susceptibility measurements it was suggested that the magnetic ground state might be a reentrant spin glass [22], but later it was recognized that the low temperature magnetic irreversibilities are not related to chemical or structural disorder.

The bulk magnetic properties for the whole series of compounds $Fe_{1-x}Cu_xCr_2S_4$ are summarized in references [2, 10, 11]. Recent results for $0 \leq x \leq 0.5$, including heat capacity data, can be found in [23]. It is generally assumed that the collinear ferrimagnetic spin structure found by neutron diffraction in $FeCr_2S_4$ holds for all $Fe_{1-x}Cu_xCr_2S_4$ intermetallics with $x < 1$ over their full LRO regime. Neutron diffraction data at a few different temperatures below T_C (i.e. 300, 200, 4 K) exist only for $Fe_{0.5}Cu_{0.5}Cr_2S_4$ [24]. They corroborate the simple ferrimagnetic spin state at the temperatures measured. The magnetic transition temperatures [11] first rise sharply from 166 to 347 K between $x = 0$ and $x = 0.5$, then remain nearly constant up to $x = 0.9$, and another rise leads finally to 376 K for $x = 1$. The rise in transition point is coupled to weaker CMR behavior. Somewhere on the approach to $x = 1$ a change from ferrimagnetism to ferromagnetism must occur when the Fe concentration on the A site becomes so low that LRO can no longer be sustained. Reliable information concerning the concentration x where the switch to ferromagnetism occurs does not exist. It has been suggested that, judging from its susceptibility curves, the spinel with $x = 0.7$ is already ferromagnetic [10], but the authors also remark that the transition from ferrimagnetic to ferromagnetic spin order is not a simple one. Orbital ordering occurs only in $FeCr_2S_4$.

The present work gives a summary of our μSR studies of four $Fe_{1-x}Cu_xCr_2S_4$ compounds ($x = 0, 0.2, 0.5, 0.8$) with respect to their local magnetic properties like the interstitial field and the fluctuation rates of the magnetic spins. The μSR method is particularly sensitive to small variations and local spin disorder in LRO spin arrays. In particular, it possesses a unique spectral response to spin glass magnetism [25]. Also unique is its sensitivity to rather slow spin fluctuations [26]. These features make it a valuable tool for the study of frustrated magnetic structures. Short reports on studies of $FeCr_2S_4$ and $Fe_{0.5}Cu_{0.5}Cr_2S_4$ have been published previously [27, 28]. We recapitulate these findings in order to present a complete picture for the whole $Fe_{1-x}Cu_xCr_2S_4$ series. In some cases, additional Mössbauer data were taken to provide further information on the magnetic properties of the Fe sublattice.

2. Experimental details

The polycrystalline powder material was prepared by solid state reactions from high purity elements. The single-phase quality of the material was confirmed by x-ray diffraction. All samples were characterized by magnetic susceptibility measurements. The powder was pressed between thin aluminized Mylar foils and positioned in the center tube of a helium-flow cryostat. This sample mounting within the helium flow ensured proper and uniform temperatures. The temperature stability was better than 0.05 K. The μSR spectra were recorded with surface muons in zero applied field (ZF) and weak transverse fields (TF) between 5 and 300 K. To suppress the background signal from muons stopped outside the sample, the 'VETO' mode [29] was enabled. The time resolution was 1.25 ns and the initial spectrometer dead time was ∼5 ns.

Details of the μSR technique are available in the literature, e.g. [26, 30–33]. Fully spin polarized muons are implanted into the sample material. They quickly come to rest at an interstitial lattice site, keeping their spin polarization intact. The muon stopping site is *a priori* not known; its

determination requires, in general, single-crystal data. Except in very pure metals, the muon rests at its stopping site in the temperature range of interest here. The muon decays with a mean life of $\tau_\mu = 2.2\ \mu$s, emitting a positron preferentially in the momentary direction of the muon spin. The μSR spectrum is the plot of the measured backward–forward (with respect to the muon beam axis) positron count rate asymmetry $A(t)$ versus time, where $t = 0$ is the moment of muon implantation into the sample. It can be expressed as

$$A(t) = A_0 G(t). \tag{1}$$

Here A_0 is the initial ($t = 0$) asymmetry (typically: $A_0 \approx 0.2$). $G(t)$ is the μSR spectral function containing information on the magnitude, the static distribution and the temporal behavior of the interstitial magnetic field B_μ created by the magnetic moments surrounding the stopped muon and/or by an externally applied field. The measured properties of B_μ can be rather directly related to corresponding properties of the magnetic spin system. One should keep in mind that μSR is not a scattering method working in reciprocal space. It is thus unable to give direct information on the geometry of the spin lattice. Yet, the μSR spectrum may exclude certain suggested forms of spin arrangement.

In an LRO magnetic system, the stopped muon ensemble sees a mean magnetic field B_μ which is termed the interstitial field. The μSR spectral function under ZF conditions for a powder material is then given (with a few special exceptions) by

$$G^{\mathrm{ZF}}_{\mathrm{LRO}}(t) = \tfrac{2}{3}\exp(-\lambda_{\mathrm{trans}}t)\cos(2\pi\nu_\mu t + \varphi) + \tfrac{1}{3}\exp(-\lambda_{\mathrm{long}}t). \tag{2}$$

The powder average has been taken care of by assuming that in 2/3 of the cases B_μ is oriented perpendicular to the muon spin and in 1/3, it is oriented parallel. The perpendicular orientation of B_μ induces spontaneous Larmor precession of the muon spin with $\nu_\mu = (\gamma_\mu/2\pi)B_\mu$ where γ_μ is the muon gyromagnetic ratio ($\gamma_\mu/2\pi = 135.5$ MHz T^{-1}). The spontaneous Larmor oscillations are damped with the rate λ_{trans}, which has its source predominantly in a static distribution of the interstitial field around its mean value B_μ. The field distribution arises from the fact that individual muons feel slightly different fields at their stopping sites even when they are crystallographically or magnetically identical. A likely mechanism is small random variations in orientation, position or magnitude of the magnetic moments in the LRO spin structure. Without going into details about the shape of the field distribution, we take $\Delta B_\mu = \lambda_{\mathrm{trans}}/\gamma_\mu$ as a measure of the distribution width. More expressive is the relative field distribution width $\Delta B_\mu/B^0_\mu$, where B^0_μ stands for the saturation ($T \to 0$) value of the interstitial field. It is a direct indicator of the degree of perfection of the LRO spin array.

Larmor precession cannot occur in the case of parallel orientation of B_μ. One only observes muon spin relaxation with rate λ_{long}, caused by the dynamics of the magnetic moments generating B_μ. One finds [34] within the strong collision model

$$\lambda_{\mathrm{long}} \propto 1/\tau_{\mathrm{s}}$$

with $1/\tau_{\mathrm{s}}$ being the fluctuation rate of the magnetic spins. The condition $\lambda_{\mathrm{long}} \ll \lambda_{\mathrm{trans}}$ is usually fulfilled. One expects in regular situations $\lambda_{\mathrm{long}} \to 0$ for $T \to 0$, i.e. that the magnetic spins become static. Included in equation (2) is a phase factor φ in the transverse term. Ideally one should have $\varphi = 0$, but small values of φ may arise from slight misalignment of the forward–backward detectors. Large values of φ, however, are an indication that a simple cosine oscillation does not properly reflect the actual motion of the muon spins under the action of B_μ. A more elaborate oscillatory term has to be used (e.g. a Bessel function). The effect of nuclear dipoles is in general insignificant in the presence of LRO magnetism.

In the paramagnetic state, the mean local field $B_\mu = 0$. In ZF, only muon spin relaxation is seen.

$$G^{\mathrm{ZF}}_{\mathrm{pm}}(t) = \exp(-\lambda_{\mathrm{pm}}t). \tag{3}$$

For λ_{pm}, where the fast fluctuation limit is valid, one has, (in contrast to λ_{long} where the slow fluctuation limit is valid),

$$\lambda_{\mathrm{pm}} \propto \tau_{\mathrm{s}}.$$

Characteristic is a sharp rise of λ_{pm} on the approach from above to a second-order magnetic phase transition. It originates from the critical slowing down of magnetic moment fluctuations (increase of τ_{s}).

Additional weak transverse field data (TF = 3 or 5 mT) were taken at various temperatures for all compounds, but will not be discussed. They were used to determine the initial asymmetry $A(0)$ and to check for the presence of a background signal. No such signal was found in any of the measurements, as is expected when the VETO mode is enabled. TF data are also helpful in fixing a magnetic transition temperature.

3. Results

3.1. $FeCr_2S_4$ ($x = 0$)

The transition from paramagnetism into LRO occurs around 170 K and so both the ordered regime and the paramagnetic regime are within the temperature range of the μSR spectrometer used.

ZF spectra taken at temperatures between 5 and 40 K are all of the form shown for the 20 K data in figure 1, left. The very early part of the spectrum which features a rapid decay of asymmetry is hidden in the initial dead time region ($\sim$0.005 μs) of the μSR spectrometer. Attempts to reproduce the spectra with the spectral function given in equation (2) failed. Performing a fast Fourier transform (FFT) on the spectral data revealed the presence of an overlay of two oscillatory patterns with different precession frequencies (figure 1, right). A two-signal least squares fit using cosine oscillations worked better, but led to excessive phase factors φ. This situation could be remedied by changing to Bessel oscillations, $J_0(2\pi\nu_\mu t)$, where J_0 is the zero-order Bessel function. A Bessel oscillation is the signature of an incommensurately modulated spin structure under the condition that the muon position is at or very near a center of local symmetry [35].

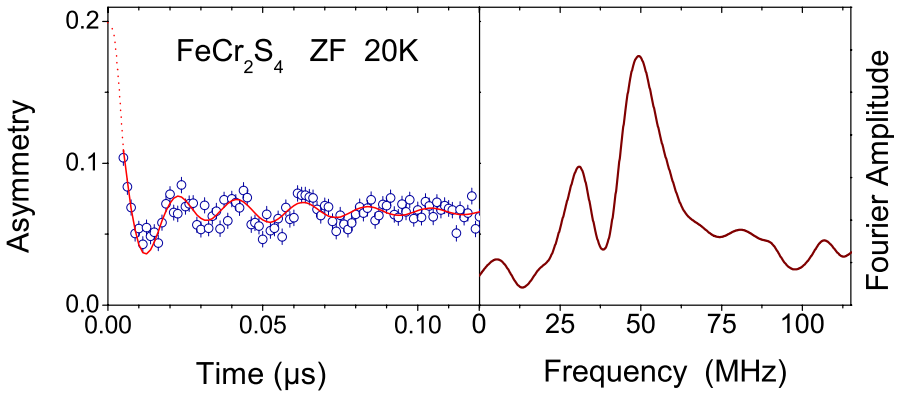

Figure 1. Left: early times part of the ZF-μSR spectrum of $FeCr_2S_4$ at 20 K. The solid line is the fit to a two-frequency Bessel oscillation pattern as discussed in the text. The broken line indicates the part of the spectrum which is lost in the instrument dead time region. This is taken from figure 4, top, in [27]. Right: FFT of the ZF-μSR spectral data. It corresponds to figure 3 in [27].

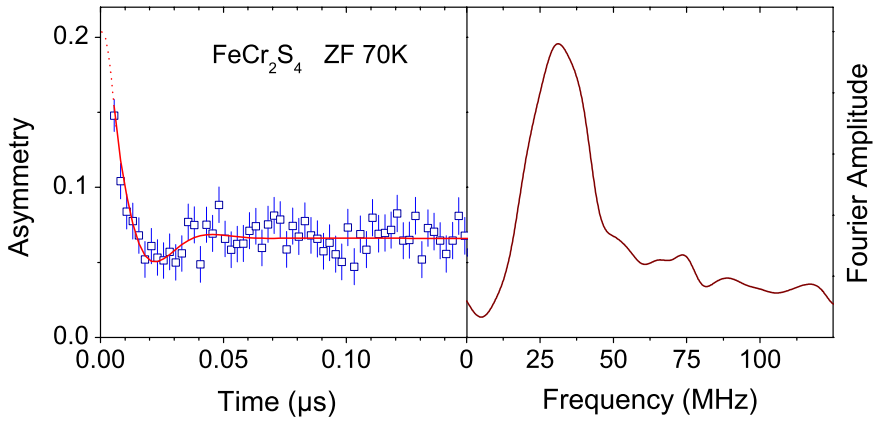

Figure 2. Left: early times part of the ZF-μSR spectrum of $FeCr_2S_4$ at 70 K. The solid line is the fit to a single-frequency cosine oscillation. A full oscillatory pattern cannot develop because of the high transverse damping rate. This is taken from figure 4, bottom, in [27]. Right: FFT of the 70 K ZF spectrum.

This is expected to be fulfilled in most cases. The Bessel pattern arises from the fact that the interstitial field B_μ has the so-called Overhauser distribution [36]. It is characterized [37] by its maximum field $B_\mu^{\max}$ which determines the precession frequency $2\pi\nu_\mu = \gamma_\mu B_\mu^{\max}$. The rather complex μSR spectra at low temperatures (see, e.g., figure 1) clearly imply that the magnetic ground state of $FeCr_2S_4$ cannot be a simple collinear ferrimagnet. In fact, μSR spectra of $Fe_{0.5}Cu_{0.5}Cr_2S_4$ taken at temperatures where more recent neutron diffraction data [24] reliably established the simple collinear ferrimagnetic state look quite different from the example shown in figure 1. They consist of a single cosine oscillatory pattern (see figure 7 in section 3.3). This simple spectral shape points, in addition, strongly toward a central position of the muon in its interstitial site.

As discussed in more detail in [27], the shape of the frequency distribution, revealed by the FFT plot of the μSR spectrum of $FeCr_2S_4$ at 20 K, is indicative of an incommensurate helical cone structure [38, 26]. The low value of $\Delta B_\mu/B_\mu^0$ (see figure 3) means that this structure is well ordered. The longitudinal relaxation rate λ_{long} remains at a low value around 0.03 μs^{-1}, but above the static limit ($\lambda_{\text{long}} \leq 0.005\ \mu s^{-1}$), pointing to the presence of weak persistent spin fluctuations.

The ZF spectra between ~40 and ~150 K can be least squares fitted by a single cosine oscillation. An example is shown in figure 2. According to what was outlined above, this result is taken as evidence that the collinear ferrimagnetic structure has been formed. The variations of λ_{long} and $\Delta B_\mu/B_\mu^0$ are depicted in figure 3 versus the reduced temperature. With the onset of the collinear ferrimagnetic spin arrangement around 40 K ($T/T_C = 0.23$), λ_{trans}, i.e. the relative field width, rises an order of magnitude, which indicates that over atomic distances the strict collinearity of the LRO ferrimagnetic spin structure is somewhat disturbed. In the discussion of the more recent neutron data [24] for $Fe_{0.5}Cu_{0.5}Cr_2S_4$, it is remarked that the fit to the Bragg peaks of the ferrimagnetic structure could be slightly improved by allowing canting of the Fe or Cr moments. A distribution of canting angles in $FeCr_2S_4$ would increase $\Delta B_\mu/B_\mu^0$. The slow rise of λ_{long} with temperature is usual behavior in an LRO magnet.

Around 150 K ($T/T_C = 0.86$) the transverse relaxation rate increases sharply, leading to values of ΔB_μ in excess

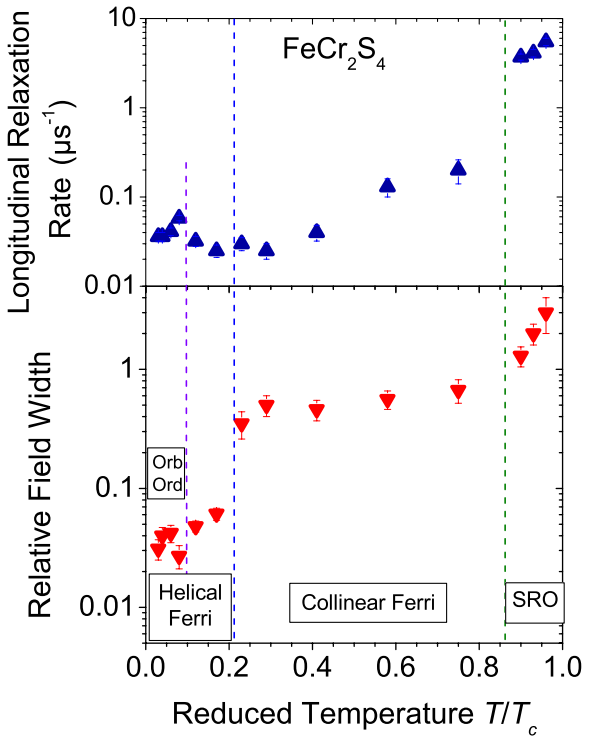

Figure 3. Dependences on the reduced temperature T/T_C of the longitudinal relaxation rate (top) and the relative field distribution width $\Delta B_\mu/B_\mu^0$ (bottom) for $FeCr_2S_4$. $T_C = 175$ K was used. One can distinguish four different magnetic regions (see the text). The raw data are the same as those used in [27].

of B_μ^0. The spin system loses its strict LRO feature and, taking into account the simultaneous massive increase of λ_{long}, is now better characterized by dynamic short-range order (SRO).

The μSR signal in the pure paramagnetic regime is a single exponentially damped pattern (equation (3)) which confirms that the muon stops at only one type of crystalline interstitial site. Spectra around the transition into paramagnetism taken in a TF of 3 mT are shown and discussed in [27] (see figures 1 and 2 therein). Their findings can be summarized as follows: above 165 K ($T/T_C = 0.94$) one observes coexistence of the SRO pattern and the paramagnetic pattern over a range of a few kelvins. The SRO signal gets rapidly smaller with rising temperature and from 175 K on, only the paramagnetic μSR signal is present. In contrast, magnetization data or Mössbauer spectra show a quite well defined second-order transition around 166 K. One reason may be the special time window of μSR for spin dynamics which is intermediate between those of Mössbauer spectroscopy and susceptibility [39, 40, 32, 30]. As discussed in the next section, $Fe_{0.8}Cu_{0.2}Cr_2S_4$ does not show this particular feature around T_C, suggesting that the special spin dynamics of the SRO state in $FeCr_2S_4$ plays a role. In section 4 we briefly discuss the possibility that the presence of a magnetic polaron could have an influence.

The transition into an orbitally ordered ground state near 10 K is not prominently visible in the μSR spectra. The small peak of λ_{long} in that temperature regime may be an indication but it is barely outside the error limit. Ordering of orbital moments mainly affects the distribution of the internal electric field to which μSR is insensitive, in contrast to Mössbauer spectroscopy. The μSR spectra taken above and below the transition into an orbitally ordered state have the same appearance and give comparable values for the two precession frequencies. Orbital ordering appears to have no significant influence on either the magnitude of the magnetic moments or their spatial arrangement. So far, μSR studies related to orbital ordering have been scarce. In the literature one finds data in connection with quadrupolar ordering [41, 42]. They mainly deal with muon Knight shift data. Such measurements require fairly large applied transverse fields. We have not performed this special type of μSR measurement.

The various ordered spin structures are indicated in figure 3.

3.2. $Fe_{0.8}Cu_{0.2}Cr_2S_4$ ($x = 0.2$)

A single well defined μSR signal is observed at all measuring temperatures. The paramagnetic spectra, especially those taken in weak TF, confirm here also that only one muon stopping site exists in the crystal lattice. Throughout the magnetically LRO regime, the ZF spectra can be least squares fitted quite satisfactorily by a single cosine oscillation function of the type given in equation (2). Examples of fitted spectra are shown in figure 4. The oscillatory pattern is not very strongly damped, giving a nearly temperature independent transverse relaxation rate of $\sim 20\ \mu s^{-1}$. This corresponds to a field distribution width of $\Delta B_\mu = 23$ mT, which is only about 6% of $B_\mu^0 = 376$ mT. In accordance with earlier discussions, this result indicates that the LRO spin structure of $Fe_{0.8}Cu_{0.2}Cr_2S_4$ is a well developed collinear ferrimagnet throughout the ordered regime (see figure 5(b)).

Mössbauer spectroscopy [43] for $x = 0.25$ established that the Fe sublattice contains Fe^{2+} and Fe^{3+}. This result is confirmed by our own Mössbauer data taken for the $x = 0.2$ material used in the μSR studies. The well defined local field seen in the μSR spectra means that the distribution of the two charge states must be fully random without any local clustering or superstructure. The Mössbauer spectra have shown that the material does not consist of macroscopic $FeCr_2S_4$ and $Fe_{0.5}Cu_{0.5}Cr_2S_4$ regions like crystalline grains, since the Fe^{2+} and the Fe^{3+} hyperfine patterns are different from those of $FeCr_2S_4$ and $Fe_{0.5}Cu_{0.5}Cr_2S_4$. The μSR results extend the homogeneity to the atomic scale.

From the temperature dependence of the field at the muon site (figure 5(b)) a Curie temperature $T_C = 247 \pm 1$ K is derived, which is close to the values given by [10, 11]. No coexistence of paramagnetic and LRO spectra in the vicinity of the Curie temperature is seen. Furthermore, both the A-site and the B-site sublattices order at the same temperature since no irregularity is observed in $B_\mu(T)$.

Figure 6 depicts the temperature dependence of λ_{long} which directly mirrors the behavior of the fluctuation rate of the magnetic moments. It shows an unexpected peak around 220 K. As discussed in section 3.3, the temperature

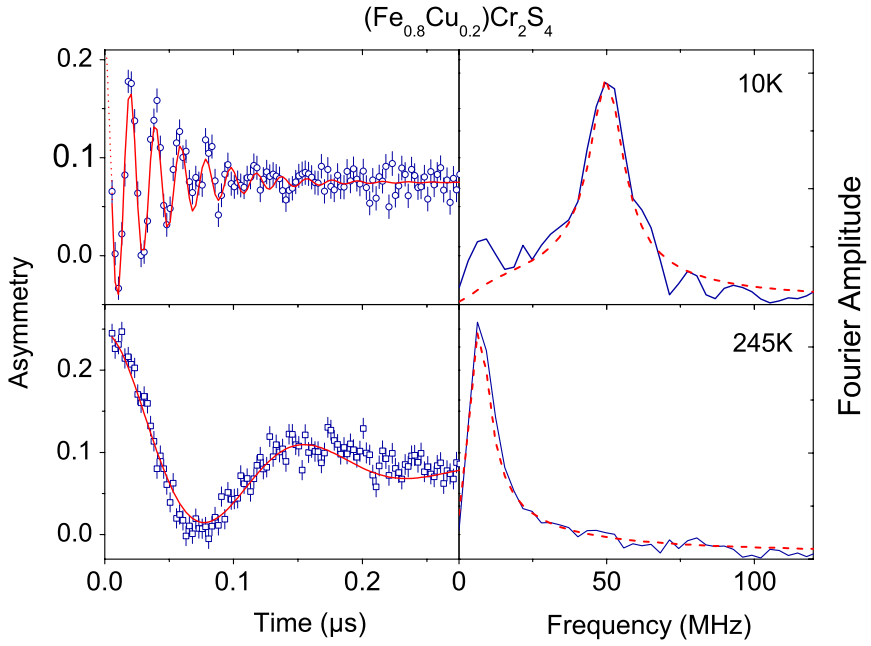

Figure 4. Left: ZF spectra of $Fe_{0.8}Cu_{0.2}Cr_2S_4$ at 10 K (the lowest temperature measured) and 245 K (the last temperature point below the magnetic transition). The solid curve is the least squares fit based on equation (2). Right: FFT of the spectral data (solid line) and of the function fitted to the spectral data (dashed line).

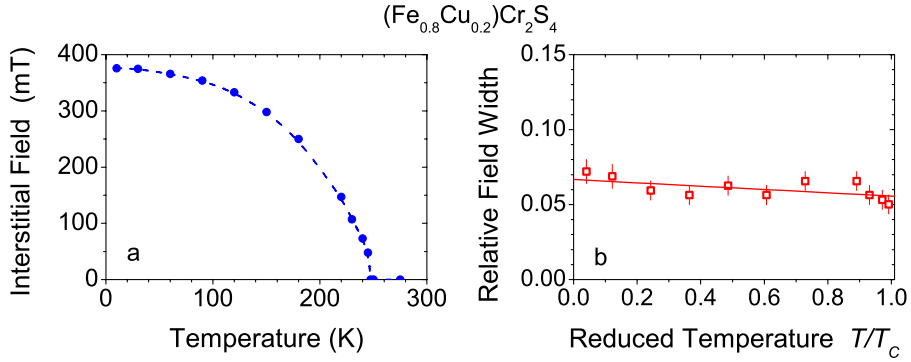

Figure 5. $Fe_{0.8}Cu_{0.2}Cr_2S_4$: (a) temperature dependence of the interstitial field. The dashed line is a guide to the eye and not a least squares fit to a Brillouin type function. (b) Dependence of the relative field distribution width $\Delta B_\mu/B_\mu^0$ on the reduced temperature T/T_C with $T_C = 247$ K. The solid line is a linear fit.

dependence of λ_{long} in $Fe_{0.5}Cu_{0.5}Cr_2S_4$ can be successfully reproduced by the theoretical function proposed in [44]:

$$\lambda_{long}(T) = CT^2 \ln T. \quad (4)$$

Here, in $Fe_{0.8}Cu_{0.2}Cr_2S_4$, the situation is different. For one thing, the increase of λ_{long} in the temperature range between 90 and 200 K is too fast to be described by equation (4). Another deviation from the predictions of equation (4), and in general a quite uncommon behavior, is the marked decrease of λ_{long} on approach to T_C. It might indicate a change in spin wave properties. Finally, while equation (4) predicts a smooth decrease of λ_{long} to zero for $T \to 0$, the spin fluctuations in $Fe_{0.8}Cu_{0.2}Cr_2S_4$ in the low temperature regime ($T < 50$ K) remain essentially constant slightly above the static limit. This presence of persistent spin fluctuations means, like in $FeCr_2S_4$, that the ordered spins experience magnetic frustration. The weak peak in λ_{long} around 12 K cannot be guaranteed within the present data accuracy.

In short, the μSR spectral data of $Fe_{0.8}Cu_{0.2}Cr_2S_4$ are compatible with a collinear commensurate simple ferrimagnetic order, stable throughout $T < T_C$. An unusual feature is the spin dynamics on approaching T_C from below.

3.3. $Fe_{0.5}Cu_{0.5}Cr_2S_4$ ($x = 0.5$)

Spectra were taken between 5 and 315 K, which is the upper temperature limit of the cryostat system used in the μSR spectrometer. Unfortunately this limit is well below the listed Curie temperature of approximately 347 K. Therefore we have no μSR data for the critical and paramagnetic regimes. All spectra recorded could be quite satisfactorily fitted with a single cosine oscillation pattern. Neutron diffraction [24] has established the collinear ferrimagnetic

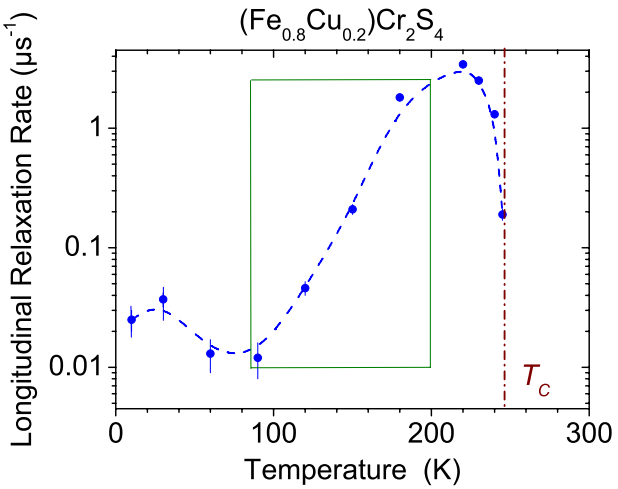

Figure 6. Temperature dependence of the longitudinal relaxation rate λ_{long} in $Fe_{0.8}Cu_{0.2}Cr_2S_4$. The dashed line is a guide to the eye. The box indicates the region with an unexpectedly fast increase in the relaxation rate with the temperature.

structure in $Fe_{0.5}Cu_{0.5}Cr_2S_4$ at 4 and 200 K. In figure 7 the corresponding μSR spectra together with their FFT are shown. As mentioned, this result forms the basis for taking a single cosine oscillation pattern in spectra of $Fe_{1-x}Cu_xCr_2S_4$ as the signature of collinear ferrimagnetism. The neutron data also establish that the temperature dependences, in particular the ordering temperatures, are identical for the two ferromagnetic sublattices.

Figure 8, left, depicts the temperature dependence of the interstitial field. Here, a discontinuous behavior is seen. Below 90 K, $B_\mu(T)$ follows closely the bulk magnetization curve, exhibiting the expected Brillouin-like behavior. Then, above ~90 K, the interstitial field suddenly drops, and finally recovers slowly to reach at ~200 K once more roughly the magnetization curve. Neither the magnetization nor the ^{57}Fe hyperfine field from our own Mössbauer data (see the inset to figure 8, left) show irregularities in that temperature range, implying that the magnitude of the magnetic moments remains unaltered. The interstitial field sensed by the muons is, however, also sensitive to the spatial orientation of the moments surrounding the muon due to the dipolar coupling. The behavior seen in $B_\mu(T)$ then points to a spin reorientation transition. As discussed more thoroughly in [28], the type of behavior seen in figure 8, left, has indeed previously been observed in other magnetic materials with established spin reorientation transitions. A notable case is that of Gd metal [45, 30], for which the availability of a single-crystal specimen allowed a very careful analysis.

Figure 8, right, shows the temperature variations of the relative field distribution width, derived from λ_{trans}, and the magnetic moment fluctuation rate as seen from λ_{long}. The behavior shown is analogous to that of Gd metal as well. In the spin reorientation region the field distribution width goes through a maximum, signaling that at the beginning of the reorientation process the canting angle is widely distributed, but finally becomes more uniform. Unfortunately, the neutron study [24] does not cover the temperature region where μSR detected a spin reorientation, and independent verification is not available. However, it mentions the possibility of canting of the Fe or Cr moments at the temperatures measured (4, 200, 300 K). The rise in the field distribution at higher temperatures is a common effect observed in magnetic materials on approach of the transition temperature to the paramagnetic state.

The temperature variation of the spin dynamics is smooth. The spin reorientation is not coupled to additional spin fluctuations. The overall temperature dependence of λ_{long}

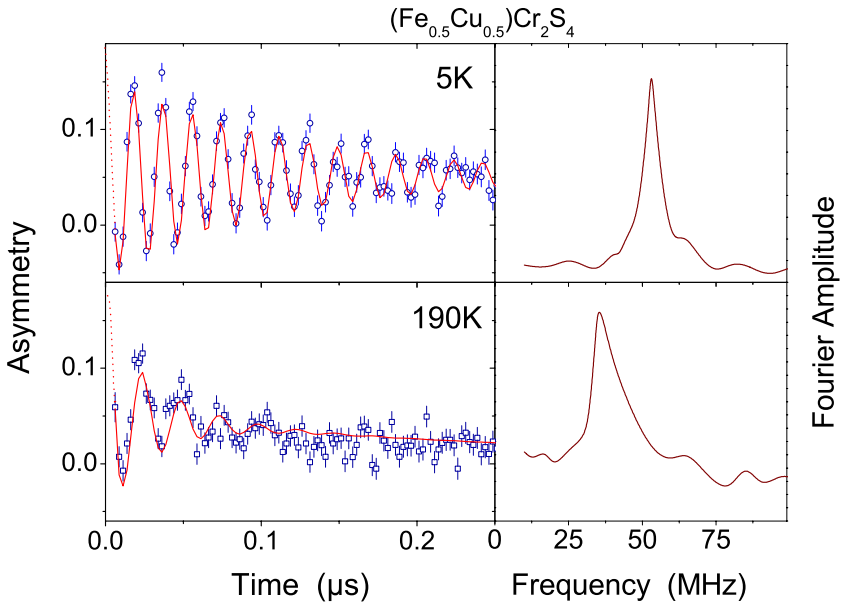

Figure 7. μSR spectra of $Fe_{0.5}Cu_{0.5}Cr_2S_4$ with their FFT at temperatures where the collinear ferrimagnetic structure has been established by neutron diffraction. The solid lines are least squares fits to a single cosine oscillatory pattern. This is taken from figure 2 in [28].

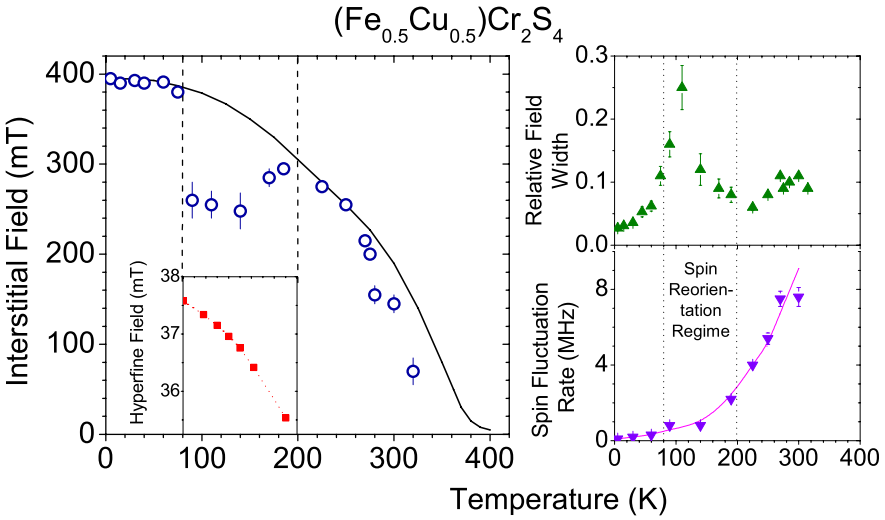

Figure 8. Left: temperature dependence of the interstitial field B_μ (open symbols). The solid line shows the temperature dependence of the magnetic susceptibility adjusted to B_μ^0. The box shows the hyperfine field (closed symbols) derived from ^{57}Fe Mössbauer measurements on material from the μSR sample. Right: temperature dependences of the relative field distribution width $\Delta B_\mu / B_\mu^0$ and the longitudinal relaxation rate λ_{long}. The solid line in the lower panel is a fit to the function equation (4). The plots are taken from figure 3 and in part from figure 4 of [28].

could well be fitted with the model for ferromagnetic spin structures developed by [44], leading to equation (4). It is possible that here λ_{long} also drops near T_C, as has been observed in $Fe_{0.8}Cu_{0.2}Cr_2S_4$. The presence of that effect here depends on a single data point and hence cannot be determined with any accuracy. The range of variation of λ_{long} with the temperature is larger in $Fe_{0.5}Cu_{0.5}Cr_2S_4$ than in the other three alloys investigated and may be an indication of the instability of the spin lattice.

3.4. $Fe_{0.2}Cu_{0.8}Cr_2S_4$ ($x = 0.8$)

A fundamental question concerning this compound is that of whether the low iron content allows magnetic LRO of the A sublattice at all. If not, the compound would be a ferromagnet like $CuCr_2S_4$, the endpoint of the series. Ferromagnetism in $Fe_{0.2}Cu_{0.8}Cr_2S_4$ had been suggested in [10]. Unfortunately, μSR cannot be used to unambiguously distinguish between ferromagnetic and ferrimagnetic order. However, the additional ^{57}Fe Mössbauer spectrum taken at 4 K and presented in figure 9 definitely exhibits substantial magnetic hyperfine splitting and hence indicates that the iron-containing A sublattice is magnetically long-range ordered.

Since $T_C \sim 350$ K [11], the μSR data are once more limited to the lower temperature parts of the LRO regime. All spectra could be fitted with single cosine oscillations. Examples are depicted in figure 10, both with high time resolution (to show the oscillatory pattern) and with low time resolution (to show the dynamic relaxation process). Basically, the spectra are consistent with simple ferrimagnetic order, according to the arguments presented in the case of $Fe_{0.5}Cu_{0.5}Cr_2S_4$.

Several unusual features, however, appear in $Fe_{0.2}Cu_{0.8}Cr_2S_4$ data with respect to the temperature

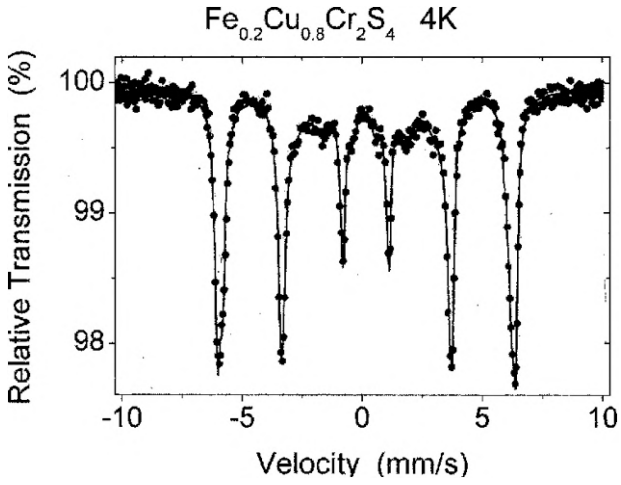

Figure 9. Mössbauer spectrum of $Fe_{0.2}Cu_{0.8}Cr_2S_4$ at 4 K. The solid line is a fit to three six-line patterns with different hyperfine fields and quadrupole interactions, but all with the Fe^{3+} isomer shift.

dependences of the interstitial field, its distribution width and the moment fluctuation rate. As depicted in figure 11, left, the temperature dependence of the interstitial field exhibits overall smooth Brillouin-like behavior with a saturation field $B_\mu^0 \approx 400$ mT. It follows roughly the magnetization curve. However, on looking in more detail, one observes (see figure 11, right) between 60 and 90 K an irregularity in the temperature dependence of B_μ, indicating some intricate change in magnetic properties. This irregularity is also present in the magnetization curve. The observed slight reduction in interstitial field and magnetization points toward a change in magnetic moment, at least in one of the sublattices. Mössbauer measurements which could shine more light on this feature are at present not available.

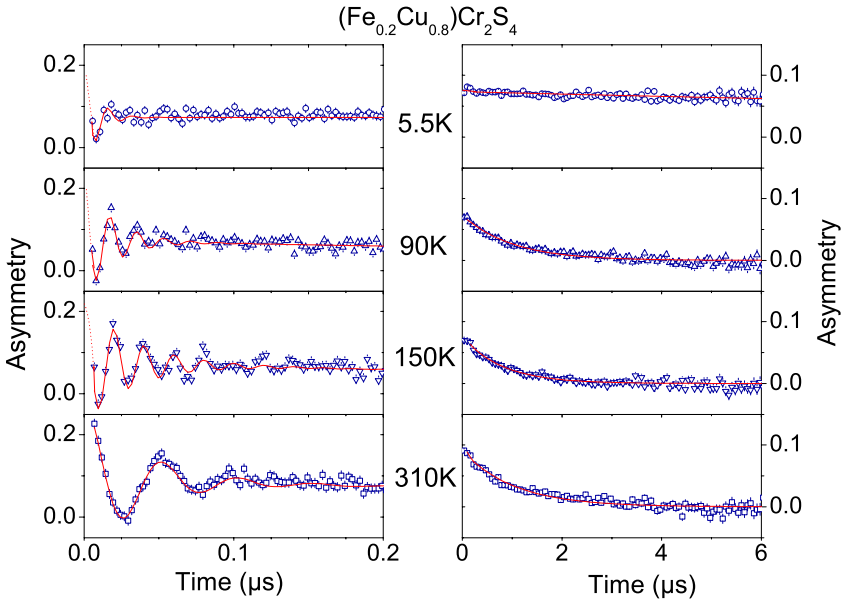

Figure 10. Typical ZF spectra of $Fe_{0.2}Cu_{0.8}Cr_2S_4$ at different temperatures within the LRO regime. The solid lines are least squares fits to equation (2). The left panels show the initial part of the spectrum in high time resolution, the right hand panels the spectra in low time resolution where only the longitudinal relaxation appears, the oscillations being averaged out.

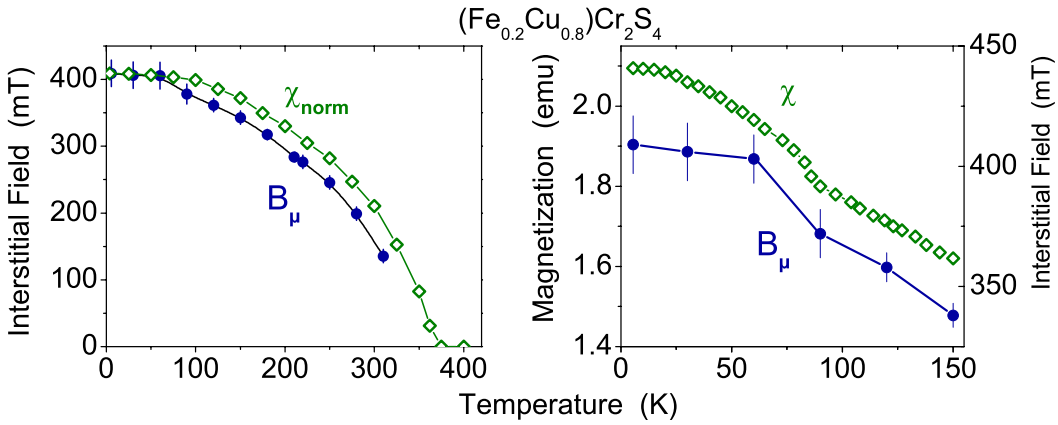

Figure 11. Left: temperature dependence of the interstitial field B_μ in $Fe_{0.2}Cu_{0.8}Cr_2S_4$ (filled symbols) and the magnetization obtained in 1 T, normalized to B_μ^0 (open symbols). Right: details of the temperature variation of the interstitial field and the magnetization in the region around 100 K, to emphasize the weak irregularity discussed in the text.

The unusual variations with temperature of the relative field width $\Delta B_\mu/B_\mu^0$ (from λ_{trans}) and the moment fluctuation rate $1/\tau_s$ (from λ_{long}) are plotted in figure 12. As regards λ_{trans}, one notices immediately just by looking at the spectra shown in figure 10 that the damping of the spin precession pattern is high at low temperatures but decreases substantially if the temperature is raised. Generally one observes the opposite behavior. As mentioned, the spectral shape is throughout consistent with simple ferrimagnetic order. Above 90 K, the size of the relative field distribution width $\Delta B_\mu/B_\mu^0 \approx 0.08$ indicates the presence of a rather well developed spin structure, which is similar to the situation in $Fe_{0.2}Cu_{0.8}Cr_2S_4$. At lower temperatures the relative field distribution width increases markedly, indicating local disturbances in the ferrimagnetic structure. One might think of small variations in the magnitude of the magnetic moments on iron initiated by differences in its local surroundings. In fact, the least squares fit to the Mössbauer spectrum depicted in figure 9 requires more than one six-line pattern. Details are at present not understood, but it shows that iron exists in the material with different hyperfine parameters.

Below 60 K, the spin system is close to static ($1/\tau_s \approx 0.02$ MHz). On elevating the temperature, it becomes suddenly dynamic and $\Delta B_\mu/B_\mu^0$ simultaneously drops to its low value discussed above. This suggests motional narrowing of the influence of the local disturbances in the magnetic structure.

4. Discussion and summary

Our μSR data demonstrate that the magnetic spin structures of the series of compounds $Fe_{1-x}Cu_xCr_2S_4$ below their well established Curie temperatures are more complex than previously anticipated. The notion of a simple collinear ferrimagnetic structure throughout the series and at all temperatures below T_C is not supported. Unfortunately, there

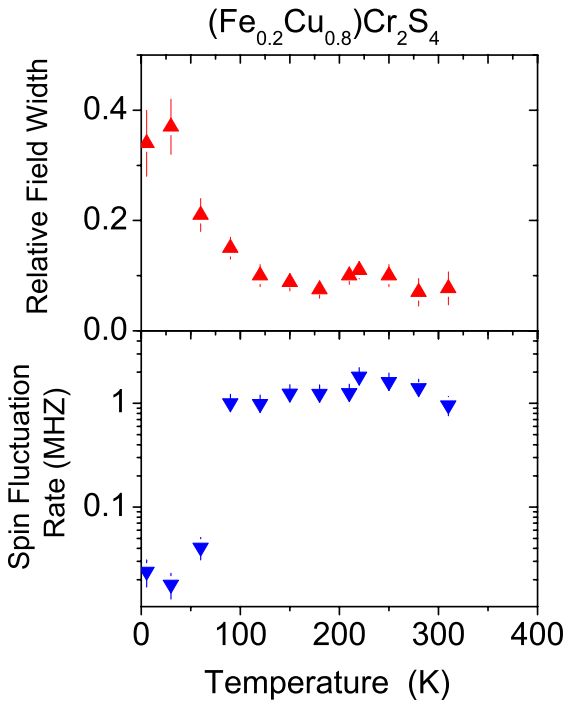

Figure 12. Temperature dependences of the relative field distribution width $\Delta B_\mu/B_\mu^0$ (top) and magnetic spin fluctuation rate $1/\tau_s$ (bottom) in $Fe_{0.2}Cu_{0.8}Cr_2S_4$.

appears no simple relation between the spin structure and the Cu concentration on the Fe sublattice.

$FeCr_2S_4$. The spin structure for the $x = 0$ compound (with only Fe^{2+} on the A site) changes with increasing temperature from a well ordered magnetically complex ground state (most likely an incommensurate helical cone structure), via a collinear ferrimagnetic state with some local spin disorder, to a dynamic SRO state. Before reaching the fully paramagnetic state, μSR observes the coexistence of SRO and paramagnetism over a narrow temperature interval. Specific heat and Mössbauer spectroscopy established orbital ordering for iron below ~10 K. This transition is not coupled to significant changes in the μSR spectra. Hence it appears that orbital ordering does not change the size of the Fe magnetic moment and has no influence on the LRO spin arrangement.

$Fe_{0.8}Cu_{0.2}Cr_2S_4$. In contrast to the case for $FeCr_2S_4$, no change in magnetic structure is seen in the μSR spectra of the $x = 0.2$ compound for $T < T_C$. The spectral shape is fully compatible with simple collinear ferrimagnetic order with very small local disorder over the whole magnetically ordered regime, despite the fact that, according to Mössbauer data, two different Fe charge states (2+ and 3+) are present. The single-frequency oscillatory pattern in the LRO regime and the single exponential decay in the paramagnetic regime demand a totally random distribution of the two Fe charge states on the A lattice site. No indication for Fe^{2+} or Fe^{3+} clusters is seen. The only abnormal feature is a drop of the fluctuation rate of the ordered magnetic moments on approach to T_C which at present is not fully understood. $Fe_{0.8}Cu_{0.2}Cr_2S_4$ is the member of the series $Fe_{1-x}Cu_xCr_2S_4$ where the simple collinear ferrimagnetic spin structure is best developed and most stable. It appears that this spin structure is stabilized by a small concentration of Cu ions in the Fe sublattice, which could ease the influence of frustration.

$Fe_{0.5}Cu_{0.5}Cr_2S_4$. The $x = 0.5$ alloy contains only Fe^{3+}. One might expect the further dilution of Fe to stabilize even more a simple ferrimagnetic order. Yet, the μSR data give evidence for an instability of the spin lattice in the form of a spin reorientation above 90 K. Still, the μSR spectra are considerably less complex than those for the $x = 0$ alloy. Spin reorientation means a collective canting of spins.

$Fe_{0.2}Cu_{0.8}Cr_2S_4$. Literature data on magnetization had suggested that the $x = 0.8$ compound is a ferromagnet like $CuCr_2S_4$. Our present Mössbauer data, however, establish that long-range magnetic order is still present in the Fe sublattice despite the high dilution with copper. The μSR spectra of $Fe_{0.2}Cu_{0.8}Cr_2S_4$ are in general compatible with ferrimagnetic order. Yet, some irregularities are seen in the temperature dependences, dramatic for the transverse and longitudinal relaxation rates, more subtle for the bulk magnetization and the interstitial field. Below 60 K the magnetic moments are essentially static, but their LRO is slightly disturbed by disorder on a short-range scale. Above 90 K the moments are dynamic and the signature for local disorder (large λ_{trans}) is reduced by motional narrowing. Between 60 and 90 K the interstitial field and the bulk magnetization show similar small deviations from the expected Brillouin-like behavior, indicating that some subtle changes take place in the LRO spin lattice. They are coupled to the sudden increase in spin dynamics.

In this paper we have not considered the possible formation of magnetic polarons associated with some fraction of implanted muons in magnetic semiconductors. In recent years, a number of papers have been published showing their existence through high transverse field μSR experiments [46–48]. The term magnetic polaron refers to a quasiparticle formed by localization of an electron from the conduction band which, due to its strong exchange interaction with magnetic ions in its immediate environment, strengthens the otherwise comparatively weak direct magnetic coupling. A fraction of implanted positive muons can form a muonium-like bound state with the localized electron. If this takes place, the probe in a μSR experiment is no longer the free muon, but now a bound polaron–muon state which could affect the μSR spectral response.

Among the compounds studied in this paper, undoped $FeCr_2S_4$ is a magnetic semiconductor. Doping with Cu increases the conductivity by an order of magnitude [23] and the $Fe_{1-x}Cu_xCr_2S_4$ compounds for $x \geq 0.2$ will provide a more metallic environment in which the magnetic polaron will not form. Since we have not performed high transverse field measurements, we do not know whether a bound muon–magnetic polaron state exists at all in $FeCr_2S_4$. But, as discussed in particular in [47], bulk magnetization in an ordered magnet suppresses the formation of a magnetic polaron. Most of our study tackles the magnetic properties of $FeCr_2S_4$ within its well established LRO magnetic regime. The situation is different just below T_C where the magnetization is very weak and above T_C where the

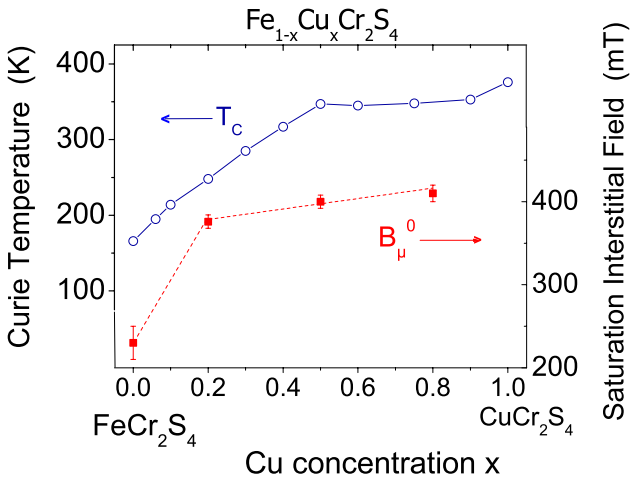

Figure 13. Influence of x on T_C from [11] (open symbols) and of the saturation interstitial field B_μ^0 (closed symbols) in $Fe_{1-x}Cu_xCr_2S_4$. The lines are guides to the eye. Since the magnetic ground state of the $x = 0$ compound is not a simple ferrimagnet, the value of its saturation field has been extrapolated from the 40 K data.

magnetization is absent in ZF. Since a magnetic polaron can be viewed as a 'ferromagnetic droplet' in the paramagnetic sea [49], this might be a cause for the observation of the coexistence of SRO and paramagnetic fractions in $FeCr_2S_4$. This unusual feature is seen neither in bulk magnetic data nor in the μSR data for $Fe_{0.8}Cu_{0.2}Cr_2S_4$, the only Cu doped sample that we could make measurements on around T_C with our experimental setup. Yet, without information on whether a muon–polaron state exists in $FeCr_2S_4$ at all, this deduction must be considered highly speculative.

To conclude, the μSR data for $Fe_{1-x}Cu_xCr_2S_4$ show that the addition of Cu on the A-site sublattice has a rather intricate influence on the magnetic exchange interaction, well beyond a simple weakening of the Fe–Fe spin coupling. The generally assumed simple collinear ferrimagnetic spin structure for the whole $Fe_{1-x}Cu_xCr_2S_4$ series appears to be stable only in $Fe_{0.8}Cu_{0.2}Cr_2S_4$. New neutron data are urgently called for to gain much needed information on the precise spin structures of the $Fe_{1-x}Cu_xCr_2S_4$ intermetallics. This would also help with theoretical treatments of the giant magnetoresistive properties which so far have been carried out predominantly for the $x = 0.5$ alloy. Remarkable also is the quite different temperature dependence of the fluctuation rates of the magnetic moments in the four $Fe_{1-x}Cu_xCr_2S_4$ alloys studied.

In contrast to the complex results for the spin structures and fluctuation rates, the dependence of the saturation interstitial field B_μ^0 on the Cu concentration is fairly straightforward. As shown in figure 13, it rises monotonically with x, as does T_C. The interstitial field increases sharply at low Cu concentrations, whereas T_C rises more slowly up to intermediate x values.

Acknowledgments

The μSR studies were performed at the Swiss Muon Source of the Paul Scherrer Institute (PSI), Villigen, Switzerland. We thank R Scheuermann, A Amato, and H Luetkens for their help in carrying out the experiments. Enlightening discussions with A Yaouanc and E Karlsson are gratefully acknowledged. This work was partly supported by the Deutsche Forschungsgemeinschaft (DFG) via TRR80 (Augsburg, Munich).

References

[1] Ramirez A P, Cava R J and Krajewski J 1997 *Nature* **386** 156
[2] Lotgering F K, van Stapele R P, van der Steen G H A M and van Wieringen J S 1969 *J. Phys. Chem. Solids* **30** 799
[3] Goodenough J B 1969 *J. Phys. Chem. Solids* **30** 261
[4] Bergman D, Alicea J, Gull E, Trebst S and Balents L 2007 *Nature Phys.* **3** 487
[5] Fritsch V, Hemberger J, Büttgen N, Scheidt E-W, Krug von Nidda H-A, Loidl A and Tsurkan V 2004 *Phys. Rev. Lett.* **92** 116401
[6] Greedan J E 2001 *J. Mater. Chem.* **11** 37
[7] Ramirez A P 2001 *Handbook of Magnetic Materials* vol 13, ed K H J Buschow (Amsterdam: Elsevier) p 423
[8] Yaouanc A, Dalmas de Réotier P, Bonville P, Hodges J A, Gubbens P C M, Kaiser C T and Sakarya S 2003 *Physica* B **326** 456
[9] Bouchard R J, Russo P A and Wold A 1965 *Inorg. Chem.* **4** 685
[10] Haacke G and Beegle L C 1967 *J. Phys. Chem. Solids* **28** 1699
[11] Tsurkan V *et al* 2005 *J. Phys. Chem. Solids* **66** 2040
[12] Haacke G and Nozik A 1968 *Solid State Commun.* **6** 363
[13] Taubitz Ch, Kuepper K, Raekers M, Galakhov V, Velea V, Tsurkan V and Neumann M 2009 *Phys. Status Solidi* b **246** 1470
[14] Kimura A, Matsuo J, Okabashi J, Fujimori A, Sishidou T, Kulatov E and Konomata T 2001 *Phys. Rev.* B **63** 224429
[15] Shirane G, Cox D E and Pickard S J 1964 *J. Appl. Phys.* **35** 954
[16] Broquetas Colominas C, Ballestracci R and Roult G 1964 *J. Physique* **25** 526
[17] Spender M R and Morrish A H 1972 *Solid State Commun.* **11** 1417
[18] Tsurkan V *et al* 2010 *Phys. Rev.* B **81** 184426
[19] Fichtl R, Fritsch V, Krug von Nidda H-A, Scheidt E-W, Tsurkan V, Lunkenheimer P, Hemberger J and Loidl A 2005 *Phys. Rev. Lett.* **94** 027601
[20] Mertinat M, Tsurkan V, Sanusi D, Tidecks R and Haider F 2005 *Phys. Rev.* B **71** 100408
[21] Maurer D, Tsurkan V, Horn S and Tidecks R 2003 *J. Appl. Phys.* **93** 9173
[22] Tsurkan V, Barau M, Szymczak R, Szymczak H and Tidecks R 2001 *Physica* B **296** 301
[23] Fritsch V *et al* 2003 *Phys. Rev.* B **67** 144419
[24] Lang O, Felser C, Seshadri R, Renz F, Kiat J-M, Ensling J, Gütlich P and Tremmel W 2000 *Adv. Mater.* **12** 65
[25] Uemura Y I, Yamazaki T, Harshmann D R, Semba M and Ansaldo E J 1985 *Phys. Rev.* B **31** 546
[26] Yaouanc A and Dalmas de Réotier P 2011 *Muon Spin Rotation, Relaxation, and Resonance* (Oxford: Oxford University Press)
[27] Kalvius G M, Krimmel A, Hartmann O, Wäppling R, Litterst F J, Wagner F E, Tsurkan V and Loidl A 2010 *J. Phys.: Condens. Matter* **22** 052205
[28] Kalvius G M, Hartmann O, Krimmel A, Wagner F E, Wäppling R, Tsurkan V, Krug von Nidda H-A and Loidl A 2008 *J. Phys.: Condens. Matter* **20** 252204
[29] Arsenau D J, Hitti B, Kreitzmann S R and Whidden E 1997 *Hyperfine Interact.* **106** 277

[30] Kalvius G M, Noakes D R and Hartmann O 2001 *Handbook on the Physics and Chemistry of Rare Earth* vol 32, ed K A Gschneidner *et al* (Amsterdam: Elsevier) p 55ff
[31] Lee S L, Kilcoyne S H and Cywinski R (ed) 1999 *Muon Science* (London: IOP)
[32] Karlsson E 1995 *Solid State Phenomena as seen by Muons, Protons and Excited Nuclei* (Oxford: Oxford University Press)
[33] Schenck A 1985 *Muon Spin Rotation Spectroscopy* (Bristol: Hilger)
[34] Uemura Y J 1999 *Muon Science* ed S L Lee, S H Kilcoyne and R Cywinski (London: IOP) p 85ff
[35] Yaouanc A 2012 private communication (see also [26, chapter 10, p 246ff])
[36] Overhauser A W 1960 *J. Phys. Chem. Solids* **13** 71
[37] Peretto P, Venegas R and Rao G N 1981 *Phys. Rev.* B **23** 6544
[38] Noakes D R 2002 *An Ornamental Garden of Field Distributions and Static ZF Muon Spin Relaxation Functions* http://musr.org/intro/ppt/GardenExport
[39] Dattagupta S 1989 *Hyperfine Interact.* **49** 253
[40] Uemura Y J 1989 *Hyperfine Interact.* **49** 205
[41] Schenck A, Gygax F N, Solt G, Zaharko O and Kunii S 2004 *Phys. Rev. Lett.* **93** 257601
[42] Schenck A, Gygax F N, Andreica D and Ōnuki Y 2003 *J. Phys.: Condens. Matter* **15** 8599
[43] Klencsár Z, Kuzmann E, Homonnay Z, Németh E, Virég I, Kühlberger M, Gritzner G and Vértes A 2005 *Physica* B **358** 93
[44] Dalmas de Réotier P, Gubbens P C M and Yaouanc A 2008 *J. Phys.: Condens. Matter* **16** S4687
[45] Hartmann O, Karlsson E, Wäppling R, Asch L, Henneberger S, Kalvius G M, Kratzer A, Klauss H-H, Litterst F J and de Malo M A C 1994 *Hyperfine Interact.* **85** 251
[46] Storchak V G, Brewer J H, Russo P L, Stubbs S L, Parfenov O E, Lichti R L and Aminov T G 2010 *J. Phys.: Condens. Matter* **22** 495601
[47] Storchak V G *et al* 2009 *Phys. Rev.* B **80** 235203
[48] Storchak V G *et al* 2009 *Physica* B **404** 899
[49] von Molnár S and Stampe P A 2007 Magnetic polarons *Handbook of Magnetism and Advanced Magnetic Materials, Spintronics and Magnetoelectronics* vol 5, ed H Kronmüller and S Parkin (New York: Wiley)